ChemPubSoc Europe

DOI: 10.1002/slct.201801730

Chemistry SELECT Communications

Catalysis

# Development of Easily Separable ZnO-Supported Au Nanocatalyst for the Oxidative Esterification of Alcohols and Reduction of Nitroarenes

Sunil M. Galani,[a, c] Arnab K. Giri,[b] Subhash C. Ghosh,*[a, c] and Asit B. Panda*[b, c]

A simple and practical protocol is described for the reduction of aromatic nitro compounds and the oxidative esterification of alcohols by using a recyclable 3D assembled porous rectangular ZnO nanoplates supported gold nanocatalysts (Au/ZnO) under mild conditions. The support 3D assembled ZnO plate was synthesized simple strategy without employing any toxic reductants or capping agents and Au was loaded through simple impregnation method. The synthesized catalyst was characterized by powder X-ray diffraction (XRD), X-ray photoelectron spectroscopy (XPS), electron microscopic study (TEM & SEM), diffuse reflectance spectrum (DRS). The developed catalyst showed excellent catalytic activity for both the reaction and ended with good to excellent yield, up to 97% yield for nitro reduction and 90% yield for oxidative esterification. The catalyst is recyclable for a minimum five times without any significant loss in catalytic activity. The catalytic activities are superior or sometime comparable to that of the reported catalyst. The use of a developed catalyst is beneficial for of low cost and availability of good support ZnO and advantageous with respect to that of separation, easily separable by simple filtration due to the bigger size of support ZnO.

Nowadays sustainable organic synthesis activity involving benign alternatives have been received tremendous attention and find notable opportunity to make important contributions in different fine chemical industries, pharmaceuticals, and also in academic research.[1] Sustainable development became an ultimate challenge of present frontiers research due to its tremendous contributions towards environmental protection, economic and societal development. Thus, the development of simple, efficient, and environmentally benign synthetic procedures, which significantly minimizes the use of toxic and hazardous starting materials as well as solvent, and atom economic, are highly demanding.[2] The general sustainable approach, prefer a method without catalyst and solvent or use of water as a solvent, but it is not applicable for most of the organic transformation reactions, and mostly applied the homogeneous molecular catalyst to get the desired product.[2] Use of a reusable heterogeneous catalyst is the possible effective way towards the sustainable development.[3] Thus, development of efficient heterogeneous catalysts, which are particularly reusable, eliminate or reduce the use of costly and hazardous substances and generate nominal waste, is highly desirable.[4]

In the recent years, nanocrystalline metal nanoparticles, particularly noble metal (Pd, Pt, and Au) based catalysts have become an integral part of the catalytic transformations.[5] However, their direct use is challenging, as noble metal nanoparticles have high chances of agglomeration, which reduced the accessible active sites and also, enhanced the particle size (grain growth). As a result, reactivity gradually decreases and often required an excess amount, thus uneconomical. In this regards, supported solid nanocatalyst, immobilized metal nanoparticles on the surface of inert/reactive supports have been developed, showed improved activity compared to that of pristine metal and generally used for different organic transformation.[6] Particularly, supported-gold nano-catalysts have been developed an exceptional interest among noble metals for its versatile and improved catalytic activity towards different organic synthesis.[7] Supported gold catalysts can be prepared easily through simple deposition–precipitation and among others with precise, controllable size and shape.[6a, 7b, 8]

Here it is important to mention that support also plays a crucial role in the catalytic activity and overall utility. The activity is dependent on its surface area, metal–support interaction, additional functionality to promote the reaction, and so-on.[9] As the catalytic activity is a surface phenomenon and metal nanoparticles are dispersed on the surface of the support, so support with the high surface area is always desirable for better activity. Further, one of the main obstacles of such active catalysts is their separation from the mixture

[a] S. M. Galani, Dr. S. C. Ghosh
Natural Products and Green Chemistry Division, Central Salt and Marine Chemicals Research Institute (CSIR-CSMCRI), G.B. Marg, Bhavnagar-364002, Gujarat, India
Tel: +91-2782567760
Fax: +91-2782567562
http://subhashghosh.wixsite.com/scghoshgroup
E-mail: scghosh@csmcri.res.in
[b] A. K. Giri, Dr. A. B. Panda
Inorganic Materials and Catalysis Division, Central Salt and Marine Chemicals Research Institute (CSIR-CSMCRI), G.B. Marg, Bhavnagar-364002, Gujarat, India
E-mail: abpanda@csmcri.res.in
[c] S. M. Galani, Dr. S. C. Ghosh, Dr. A. B. Panda
Academy of Scientific and Innovative Research, Central Salt and Marine Chemicals Research Institute (CSIR-CSMCRI), G.B. Marg, Bhavnagar-364002, Gujarat, India

Supporting information for this article is available on the WWW under https://doi.org/10.1002/slct.201801730

after the reaction, as the simple filtration methods are not applicable for very small size particles and in consequence the support is bigger enough to be separated by simple filtration method. For easy separation, magnetic support has also been used, but for its inherent magnetic property, it is difficult to overcome the agglomeration. More importantly, the support should be abundant and economical.

ZnO is an inexpensive, non-toxic and abundant transition metal oxide and also investigated extensively as catalyst and support.[10] However, its surface area is very low, due to its high crystalline nature. To enhance its surface area as well as catalytic activity different attempts have been made, like a composite with graphene oxide, ZnO based MOF, a paper matrix that consisted of ceramic fibres.[11] However, their fabrication procedures are mostly complicated. In recent years, hierarchical 3D assembled porous ZnO microstructures with the high surface area have received significant importance and used for diverse applications like sensor, lithium-ion battery, and solar cell.[12] Although their use in catalysis as support is advantageous owing to the high surface area, easy separation through filtration for a bigger size, quite, unfortunately, their use in catalysis is very scared.[12a-b, 13]

In continuation of our efforts towards development of efficient nanocatalysts and corresponding sustainable and greener protocols for organic transformation,[14] Herein, we report the development of an efficient and easily separable supported catalyst Au/ZnO, Au nanoparticles supported on 3D assembled porous rectangular ZnO nanoplates, and efficient protocol for oxidative esterification of alcohols and hydrogenation of aromatic nitro compound to the corresponding amine using our developed catalyst. Reduction of nitro compound to the corresponding amine is a reliable model reaction to assess catalytic activity and also an industrially important organic transformation.[15] Esters represent an important class of organic compounds and ubiquitous building block of different fine and bulk chemicals, are also useful in a wide variety of industrial applications, such as coatings, adhesives, resins, fragrances, perfumes, plasticizers, etc. Several methods have been developed and explored for ester synthesis. Conventionally, reactions of carboxylic acids or their derivatives with alcohols in the presence of a catalyst are mostly used in industry. In the recent past, oxidative esterification of aldehydes with alcohols has received substantial attention.[16] However, owing to the easy availability and cost-effectively, direct esterification of alcohols to ester is more convenient and demanding.

## Results and discussions

### Materials characterization

The powder XRD patterns were recorded to investigate the phase and purity of the synthesized hierarchically assembled porous Au-ZnO nanostructures. Figure 1a-d represent the XRD patterns of the synthesized Au/ZnO obtained after heating at 300 °C. The XRD pattern of the 0.5 wt%, 1 wt%, 1.5 wt% Au/ZnO NPs (Figure 1a-c) exhibit well-resolved X-ray diffraction,

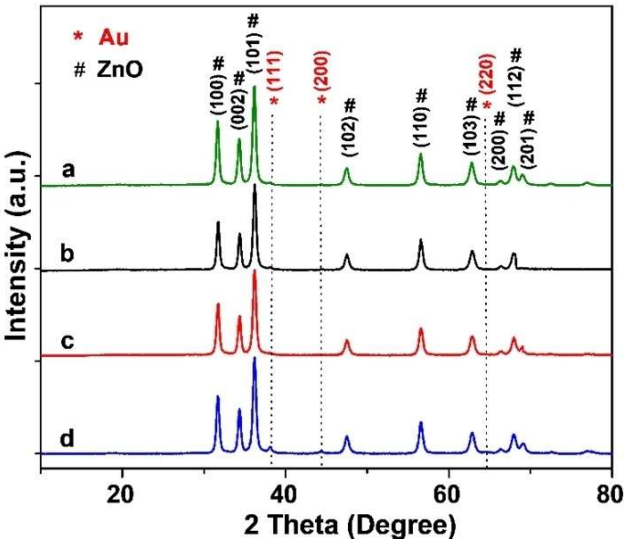


**Figure 1.** X-ray diffraction pattern of the materials; (a) 0.5 wt% Au/ZnO NPs, (b) 1 wt% Au/ZnO NPs, (c) 1.5 wt% Au/ZnO NPs and (d) 2 wt% Au/ZnO NPs

indexed to (100), (002), (101), (102), (110), (103), (200), (112) and (201) planes of the hexagonal ZnO structure (JCPDS 36-1451) which are the almost identical to that of diffraction patterns of as-synthesized Au/ZnO (Figure S1). In this XRD pattern, no peak for Au was identified, which is most probably due to the homogeneously distributed less amount of Au. However, 2 wt % Au/ZnO showed very low intense characteristic diffraction peak for (111), (200) and (220) planes of metallic Au (JCPDS No. 04-0784) in addition to the corresponding intense peaks of ZnO (Figure 1d).

Morphology of the synthesized Au loaded catalysts was determined by SEM analysis. Low-magnified SEM image indicates that the presence of 3D hierarchically assembled arrangement of rectangular plates towards a big-flower (Figure 2a) magnified images revealed that individual plates are of 2.5–3.5 μm long, 1.5-2.5 μm width and 100-150 nm thickness (Figure 2b-c). A high magnification SEM image revealed that the surface of the flakes contains irregular and open pores (Figure 2d). No distinct morphological change with bare ZnO plate was not identified.[12b] Presence of any individual particles of Au was not identified, most probably due to the smaller particle size. However, the corresponding EDX spectrum confirmed the existence of Au in the ZnO surface (Figure S2) and it also clearly evidence the presence of Au with Zn and O. The low-resolution TEM image confirms the synthesized rectangular ZnO plates are porous and the pore size is nearly between 40-60 nm (Figure 3a). The magnified TEM image the presence of a homogeneous distribution of Au nanoparticles on ZnO surface, with a particle size in between 3-4 nm (Figure 3b-c). The Au nanoparticles are of polyhedral shape. In the high-resolution TEM (HR-TEM) image, the presence of distinct lattice fringes, in both ZnO surface and Au particle, confirmed that both the Au nanoparticle and ZnO plates are highly crystalline in nature (Figure 3d). The lattice fringe spacing of 0.234 nm is in good agreement of (111) plane of fcc

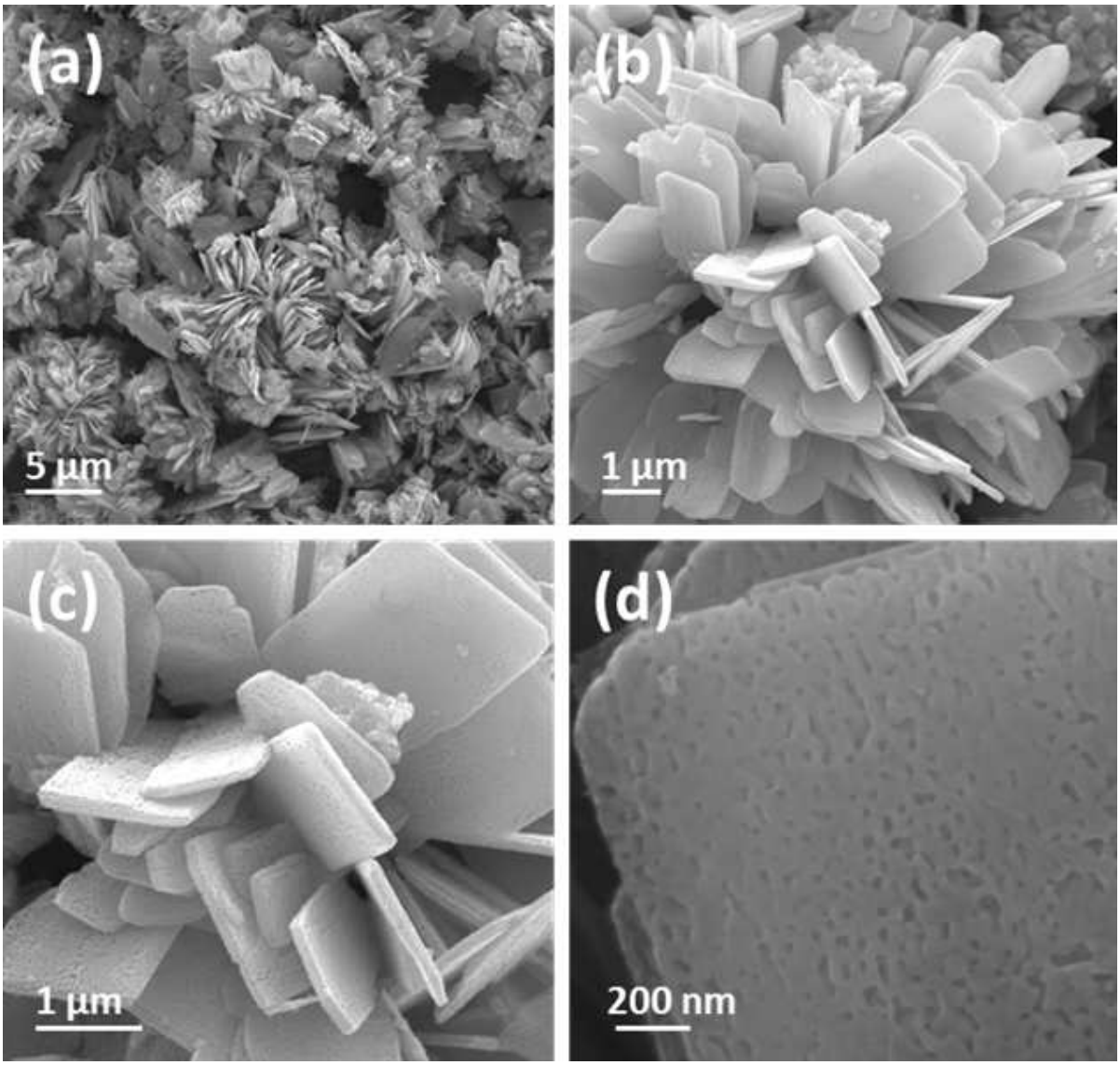


**Figure 2.** (a) SEM images of 1 wt% Au loaded/ ZnO NPs before calcinations and (b) after calcination. (c) and (d) HR-SEM images of 1 wt% Au loaded/ ZnO NPs

Au (Figure 3d). Also, the lattice fringe spacing of 0.256 nm is in good agreement with the d-spacing between the (002) plane of hexagonal ZnO (Figure 3d), which supports the XRD data. It can also be concluded that the pristine hierarchy of ZnO and the pore structure was not disturbed during the reduction of Au on ZnO plates.[12b] Figure 4 represents the Diffuse Reflectance Spectra (DRS) of pristine ZnO and calcined Au/ZnO materials. Pristine ZnO plates showed only a sharp exciton absorption band in UV region, but Au loaded samples exhibit the presence of additional broad SPR (Surface Plasmon Resonance) absorption band in the visible region, which can be ascribed to the absorption band for metallic Au, with exciton absorption band in UV for ZnO. Here it is essential to mention that SPR adsorption band in the visible region for as-synthesized Au/ZnO samples are very weak, but after heat treatment (at 300 °C) the corresponding SPR band become intense (Figure 4). This is due to the formation of metallic gold, with the increase in the Au loading a gradual blue shifting of the SPR absorption band was observed, this can be ascribed to the gradual increase in the particle size. The BET surface area of the synthesized porous Au/ZnO architecture samples is in the range of 11-15 $m^2 g^{-1}$ with a total pore volume of 0.13-16 $cm^3 g^{-1}$. All the samples possess a broad pore size distribution (15-75 nm) and support the TEM observation (Figure S3).

The survey X-ray photoemission spectrum (XPS) of 1 wt% Au/ZnO NPs showed the photoemission signatures of Zn 2p, O 1s, Zn 3p and Au 4f (Figure 5a). Corresponding, in 2p core-level spectrum of Zn, in the range of 1015-1055 eV, the two peaks in the binding energy at 1045 and 1020 eV can ascribe to Zn 2p1/2 and 2p3/2, respectively (Figure 5b). Deconvoluted core level O1s spectra evidenced the presence of three peaks at 530.2, 531.2 and 532.8 eV (Figure 5c). The peak at 532.8 eV is ascribed to the loosely bound oxygen on the surfaces of ZnO.[17] The low binding energy component appearing at ca. 530.2 eV comes

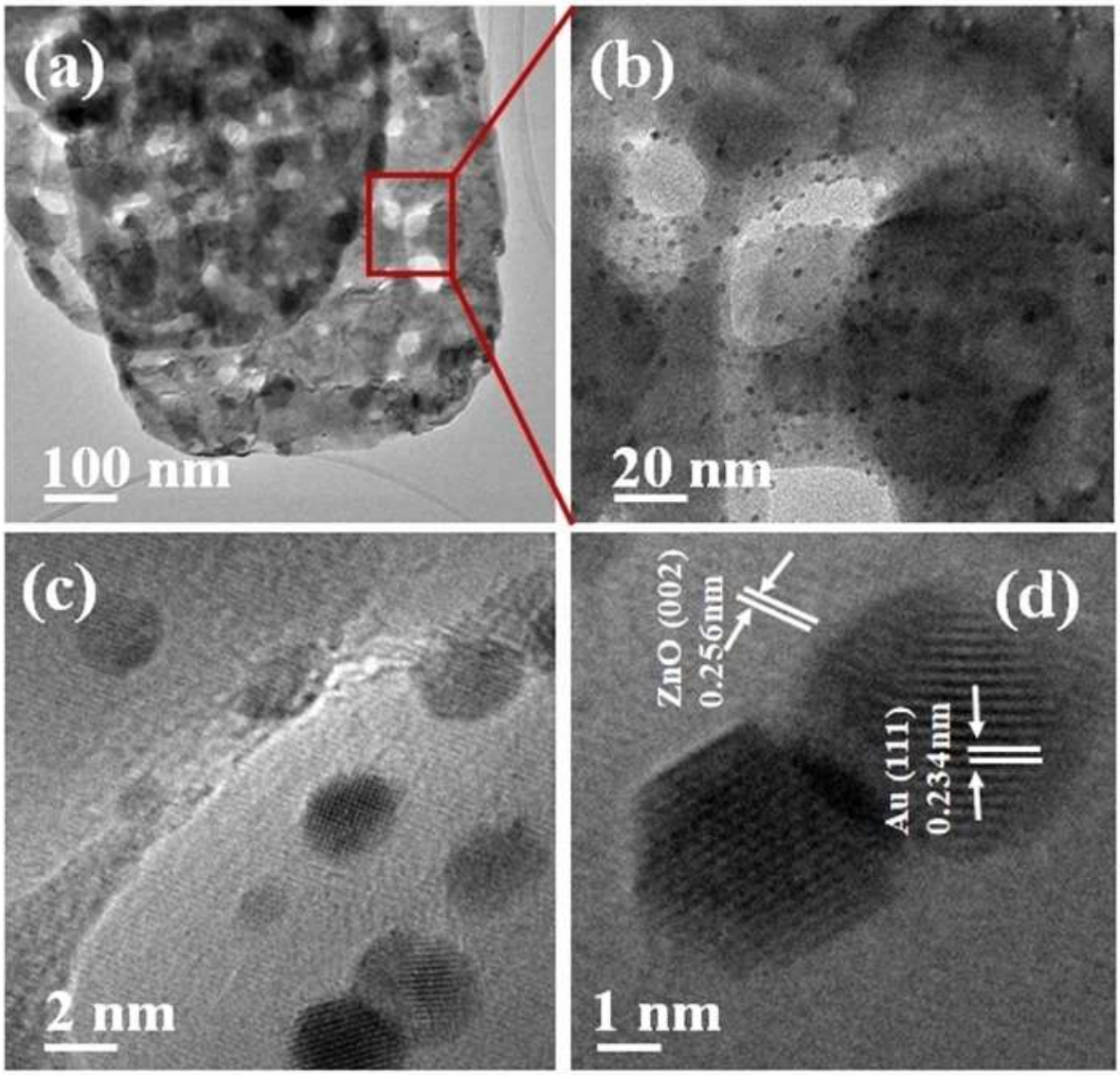


**Figure 3.** (a, b, and c) TEM images of 1 wt% Au loaded ZnO NPs and (d) HR-TEM image of polyhedral Au.

from the $O^{2-}$ ions in the wurtzite structure of the hexagonal $Zn^{2+}$ ion array.[18] The medium binding energy peak, centered at 531.2 eV, is attributed to $O^{2-}$ in the oxygen-deficient regions within the ZnO matrix.[19] The deconvoluted core level spectra in the range of 81-97 eV, showed the presence of 4 peaks, correspond to Zn $3p_{3/2}$ (88.4 eV), Zn $3p_{1/2}$ (91.1 eV), Au $4f_{5/2}$ (87.1 eV) and Au $4f_{7/2}$ (83.2 eV) (Figure 5d). The binding energy of Au 4f is found to be shifted towards slightly lower values compared to pure gold ($4f_{5/2}$, 87.71 eV, and $4f_{7/2}$, 84.00 eV).[20] A more reasonable explanation for this 0.8 eV shifting of Au $4f_{7/2}$ is the reduced size of the Au particle along with good Au/ZnO (support) interaction.[21]

## Catalytic Activity

### Nitro reduction

The catalytic activity of hierarchical Au/ZnO NPs was evaluated for the direct reduction of the nitroarenes to the corresponding amine. Initially, the reaction of 4-nitrobenzonitrile in methanol (2 mL) was carried out with 0.5 wt% Au/ZnO nanocatalyst (20 mg) in the presence of 3 eq $NaBH_4$ under an air atmosphere at 60 °C for 1 h; 53% of the desired reduced amine product was obtained (Table 1, entry 1), to our desire nitrile group remain unreacted. With 1 wt% Au/ZnO NPs, reaction works excellent and almost quantitative yield was observed (Table 1, entry 2) at room temperature, and reaction completed within 45 min. Reaction progress with time also monitored by UV-Vis spectroscopy (Figure S4). Without the reducing agent ($NaBH_4$) no product formation was observed (Table 1, entry 3). Increasing

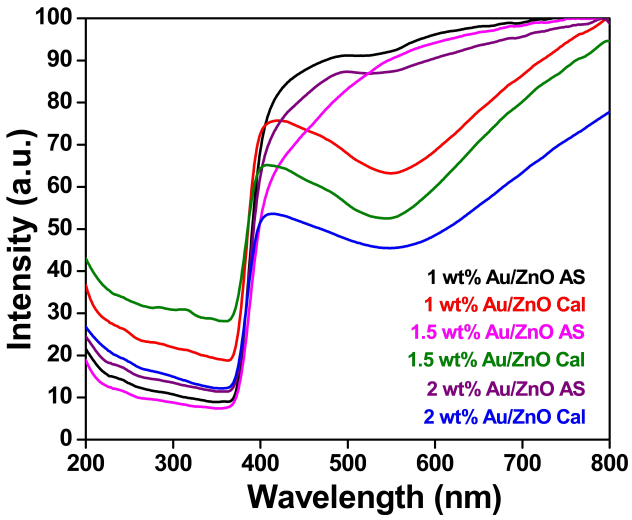


**Figure 4.** DRS spectra of the synthesized Au/ZnO NPs with varying Au loadings

**Table 1.** Optimization of the nitro reduction over Au/ZnO NPs[a]

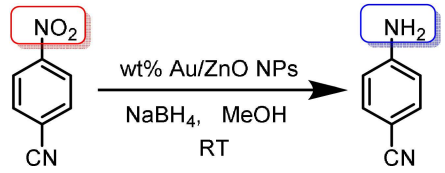


| Entry | Catalyst | Time (Min.) | $NaBH_4$ eq. | Isolated yield% |
|---|---|---|---|---|
| 1 | 0.5 wt% Au/ZnO NPs | 60 | 3 | 53 |
| 2 | **1 wt% Au/ZnO** NPs | **45** | **3** | **96** |
| 3 | 1 wt% Au/ZnO NPs | 60 | - | trace |
| 4 | 1.5 wt% Au/ZnO NPs | 45 | 3 | 96 |
| 5 | 2 wt% Au/ZnO NPs | 45 | 3 | 96 |
| 6 | - | 90 | 3 | 0 |
| 7 | ZnO nanoplates | 90 | 3 | 0 |
| 8[b] | 1 wt% Au/ZnO NPs | 60 | 3 | 67 |
| 9 | 1 wt % Au/ZnO NPs | 30 | 3 | 60 |
| 10 | 1 wt% Au/ZnO NPs | 60 | 2 | 78 |
| 11[c] | 1 wt% Au/ZnO NPs | 90 | - | trace |
| 12 | Au-NPs | 90 | 3 | 38 |

[a]Reaction condition: 1 mmol, 4-nitrobenzonitrile, 3 mmol $NaBH_4$, 20 mg catalyst, 2 mL methanol, room temp., [b] 10 mg catalyst; [c] $NH_2$-$NH_2$ as reducing agent.

the catalyst loading to 1.5 and 2 wt% similar reactivity was observed, and the reduction needs a similar time to complete, and the nitrile the group remains untouched (Table 1, entries 4-5). However, in the absence of a catalyst and simple ZnO NPs no product formation was observed, even at high reaction temperature and longer reaction time (Table 1, entries 6-7). With a lesser amount of catalyst (10 mg), the lower yield of amine was observed (Table 1, entry 8). At 30 min reaction time, we only got 60% yield, and with 2 equivalent NaBH4 inferior yields of 4-aminobenzonitrile was observed (Table 1, entries 9-10). Instead of $NaBH_4$ when hydrazine was used as reducing agent the only trace of the amount of product was obtained (Table 1, entry 11). We have also carried out the reaction with the pure gold nanoparticle, but quite, unfortunately, a diminished yield (38%) of the desired product was obtained (entry 12, see ESI for details). During the solvent screening, it was observed that water, ethanol or a mixture of ethanol/methanol-water were not compatible with this transformation (ESI, Table S1†). For nitro reduction 2 mL, methanol solvent was required to get good yield and selectivity (ESI, Table S1†, entries 3). After optimizing the reaction conditions, the catalytic efficiency of 1 wt% Au/ZnO NPs was further explored, substrates with electron donating and electron withdrawing groups at para position produced excellent yield (91% to 96%) of corresponding amine product (Table 2, 2a-2e, 2h). ortho-methyl nitrobenzene also works well, so steric factor may not have any such effect for this reaction (Table 2, 2f). 1-nitro-naphthalene also converted to amine in excellent yield (Table 2, 2g). We have found that o-nitro aniline converted to

**Table 2.** Substrate Scope of nitro compounds [a]

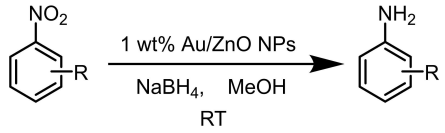


| Entry | Starting Material | | Product | | Time | Yield [%] |
|---|---|---|---|---|---|---|
| 1 | 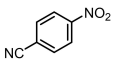 | **1a** | 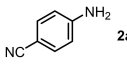 | **2a** | 45 min | 96 |
| 2 | 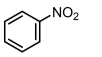 | **1b** | 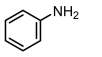 | **2b** | 1 h | 95 |
| 3 | 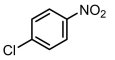 | **1c** | 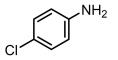 | **2c** | 1 h | 94 |
| 4 | 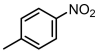 | **1d** | 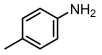 | **2d** | 1 h | 94 |
| 5 | 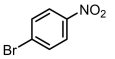 | **1e** | 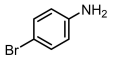 | **2e** | 1 h | 91 |
| 6 | 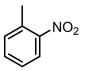 | **1f** | 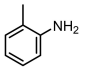 | **2f** | 45 min | 94 |
| 7 | 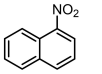 | **1g** | 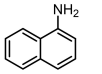 | **2g** | 1 h | 94 |
| 8 | 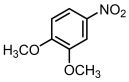 | **1h** | 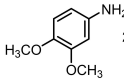 | **2h** | 2 h | 88 |
| 9 | 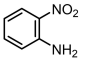 | **1i** | 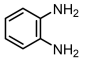 | **2i** | 2 h | 88 |
| 10 | 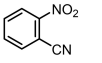 | **1j** | 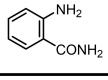 | **2j** | 1 h | 97 |

[a] Reaction conditions: Nitro compound (1 mmol, 1 eq); 1 wt% Au/ZnO NPs (20 mg); $NaBH_4$ (3 mmol, 3 eq); Methanol (2 mL); RT

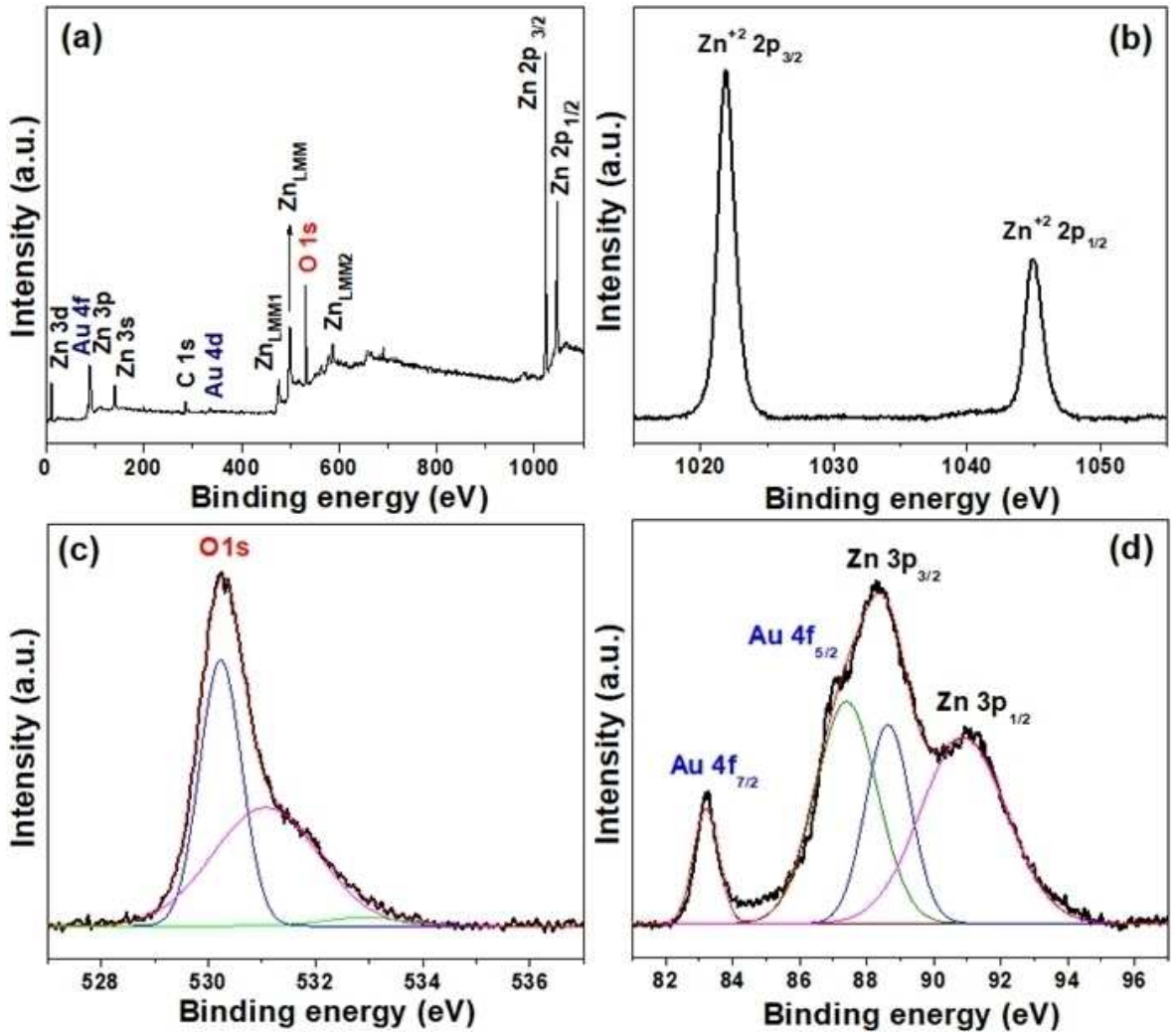


**Figure 5.** (a) XPS survey spectrum and high resolution XPS spectra of (b) Zn 2p, (c) O 1s, (d) Au 4f of 1 wt% Au/ZnO NPs arrays.

benzene 1,2-diamine (Table 2, 2i) in excellent yield (88%) and this reaction was carried out in water. When o-nitrobenzonitrile used as a substrate both nitrile and nitro group was reduced as observed by others.[22] Here also, we checked with water (2 mL) as a green solvent instead of methanol (2 mL) Moreover, the reaction goes well with excellent yield (Table 2, 2j).

### Esterification of alcohols

Encouraged by this excellent catalytic activity 1 wt% Au/ZnO NPs for reduction of nitro compounds, the catalyst was used for oxidative esterification of alcohol in the benign reaction medium. The investigation was initiated with our developed 1 wt% Au/ZnO NPs and benzyl alcohol as a model substrate in 2 mL methanol (Table 3). Initial attempt of esterification of benzyl alcohol with methanol in the presence of our catalyst at 60 °C, 15h showed only 15% of desired methyl ester product (Table 3, entry 1). We anticipated that this reaction required some base, so 20 mol% sodium carbonate was added and to our delight excellent yield of methyl benzoate was isolated (Table 3, entry

**Table 3.** Optimization of Oxidative esterification over Au/ZnO NPs [a]

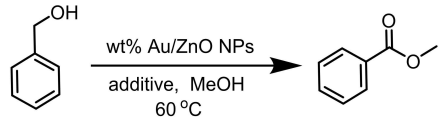


| Entry | Catalyst | Base 20 [mol%] | T [°C] | Isolated yield [%] |
|---|---|---|---|---|
| 1 | 1 wt % Au/ZnO NPs | - | 60 | 15 |
| 2 | **1 wt% Au/ZnO** NPs | **$Na_2CO_3$** | **60** | **90** |
| 3 | 1.5 wt% Au/ZnO NPs | $Na_2CO_3$ | 60 | 90 |
| 4 | 1 wt% Au/ZnO NPs | NaOH | 60 | 86 |
| 5 | 1 wt% Au/ZnO NPs | $K_2CO_3$ | 60 | 26 |
| 6 | 1 wt% Au/ZnO NPs | $NaHCO_3$ | 60 | 65 |
| 7[b] | 1 wt% Au/ZnO NPs | $Na_2CO_3$ | 80 | 90 |
| 8[c] | 1 wt% Au/ZnO NPs | $Na_2CO_3$ | 60 | 88 |
| 9[d] | 1 wt% Au/ZnO NPs | $Na_2CO_3$ | 60 | 85 |
| 10 | ZnO NPs | $Na_2CO_3$ | 60 | trace |
| 11 | - | $Na_2CO_3$ | 60 | - |
| 12[e] | 1 wt% Au/ZnO NPs | $Na_2CO_3$ | 60 | - |
| 13[f] | **1 wt% Au/ZnO** NPs | **$Na_2CO_3$** | **60** | **90** |

[a]Reaction conditions: benzyl alcohol (1 mmol); Catalyst (40 mg); additive (20 mol%); Methanol (2 mL); temp. 60 °C; time 15 h; $O_2$ balloon; [b] time 20 h; [c] Methanol 5 ml; [d] 50 mol% $Na_2CO_3$; [e] $N_2$ balloon; [f] 30 mg catalyst

2). With higher Au loading (1.5 wt%) similar reactivity was observed (Table 3, entry 3). While altering of the base was not so useful, sodium carbonate was found the superior (Table 3, entries 4-6). Next, we increase the reaction temperature to 80 °C; similar reactivity was observer and reaction completed in 12h (Table 3, entry 7). With increasing the amount of solvent and the amount of base does not have any effect on the reaction (Table 3, entries 8-9). We have run the control experiment, in the absence of a catalyst or without gold doped ZnO nanoplates no reaction was observed (Table 3, entries 10-11). It is important to mention that molecular oxygen also plays a crucial role when we carry out the reaction in under nitrogen atmosphere, no reaction takes place (Table 3, entry 12). Therefore, catalyst, base, and oxygen as oxidant all are important for this conversation. Finally, we found that lesser catalyst loading of 30 mg is showed similar reactivity (Table 3, entry 13) and It's chosen as an optimized condition for further exploration of substrate scope. We have checked with other benzyl alcohol derivatives bearing different substitution at para position, with electron donating group, like methyl, chloro, methoxy works well, and good to excellent yield of the corresponding methyl ester was observed (Table 4, 3b-3d, 83-85%). However, with

**Table 4.** Substrate Scope of esters [a]

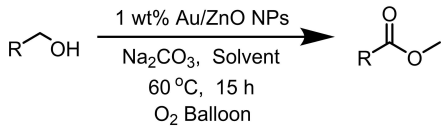


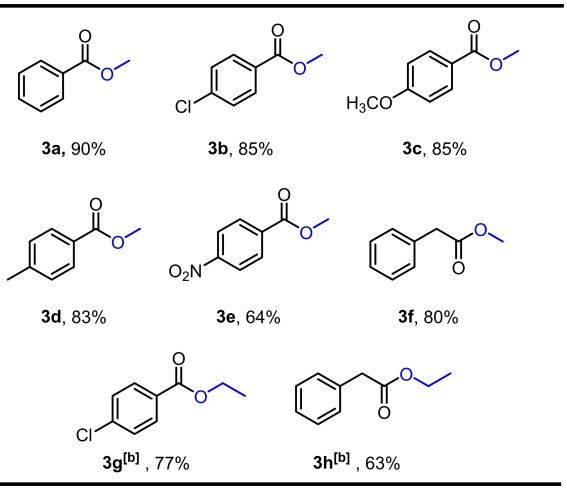


[a] Reaction conditions: Alcohol (1 mmol); 1 wt % Au/ZnO NPs (40 mg); $Na_2CO_3$ (20 mol%); Methanol (2 mL); temp. 60 °C; time 15 h; $O_2$ balloon; [b] used Ethanol instead of Methanol.

strong electron withdrawing group, a nitro group, diminished yield was observed (Table 4, 3e, 64%). To our delight, other than benzylic, when 2-phenyl ethanol was used reaction proceeds smoothly, and 80% of the desired product (Table 4, 3f) was obtained. Next, we changed the solvent from methanol to ethanol, as expected esterification proceeds well for both benzylic and non-benzylic alcohol (Table 4, 3g and 3h).

For the heterogeneous nature of the reaction, a standard leaching experiment was conducted by the simple filtration method. The model reaction of nitro reduction of 4-nitrbenzonitrile continued for 45 minutes in the presence of the 1 wt% Au/ZnO NPs at room temperature. Inductively coupled plasma atomic emission spectra (ICP-AES) analysis of the filtrate revealed the absence Au species in the filtrate. The stability of 1 wt% Au/ZnO NPs was assessed for the nitro reduction of 4-nitrobenzonitrile to the corresponding product by recycling and reuse of the catalyst five times without any significant loss of the catalytic activity. After completion of the reaction between each cycle, the 1 wt% Au/ZnO NPs catalyst could be easily separated by simple filtration, washed with ethyl acetate, dried overnight in the oven, and subjected to the next cycle. Notably, after the 5th cycle, negligible loss in the yield was observed (after the first cycle 96% and after 5th cycles 83%; see ESI, Figure S5†). The decrease in yield may be due to the adsorbed amine product on the catalyst surface which is clearly evidenced by IR spectra. (see ESI, Figure S6) The morphology of the catalyst remains quite unchanged after reusing of the catalyst after 5$^{th}$ cycle (see ESI, Figure S7) The reaction mixture colour change indicates the reduction of the nitro group to an amine group. (see ESI, Figure S8). To see the catalytic efficiency of the synthesized 1wt% Au/ZnO NPs with respect to the literature reported Au based as well as other catalyst, we have prepared two respective comparison Table (see ESI, Table S2, and S3). From the table, it is well established that the catalytic activity of synthesized 1wt% Au/ZnO NPs superior or comparable two that of the reported catalyst. However, the use of developed 1wt% Au/ZnO NPs is advantageous concerning that of separation; the catalyst is easily separable by simple filtration due to the bigger size of support 3D assembled porous rectangular ZnO nanoplates. To get the insight of the reaction mechanism, we have carried out the model nitro reduction in the presence of (2,2,6,6-Tetramethylpiperidin-1-yl)oxyl (TEMPO, the radical scavenger), the reaction proceeds smoothly, and similar yield (95%) was obtained. This observation indicates that the reaction might not follow the radical pathway.

## Conclusions

In summary, we have successfully developed 1 wt%Au loaded hierarchically assembled 3D porous ZnO as an efficient catalyst for selective reduction of nitro arenes to corresponding amines, the reaction shows good substrate group tolerance including halo, methoxy functional group with excellent yield. This reaction run under the mild and neutral condition, at room temperature and most of the reaction completed within 1h. For oxidative esterification of alcohols, this strategy provides an atom economic and environmentally benign method for the synthesis of the ester from alcohol. The catalytic activity is better or sometimes comparable with respect to the literature reported Au based as well as other heterogeneous catalyst. Finally, the use of a developed catalyst is advantageous due to its easy separation capability by simple filtration due to the bigger size of 3D assembled porous rectangular ZnO nano-

plates and extendable to other organic reaction for sustainable development.

### Supporting Information Summary

Detailed experimental procedures, materials characterization data, spectral characterization data of all new compounds; and $^{1}H$ and $^{13}C$ spectra of all compounds are available.

## Acknowledgments

*CSIR-CSMCRI Communication No. 105/2018. We are thankful to the SERB, DST, India (EMR/2016/002427 and EMR/2014/001219), for financial support for this work. Authors also acknowledge the AESDCIF-CSMCRI, for analytical services and materials characterization. SG acknowledges CSIR for providing fellowship.*

## Conflict of Interest

The authors declare no conflict of interest.

**Keywords:** 3D assembled the structure · esterification · gold nanocatalyst · nitro reduction · ZnO nanoplates

[1] a) W. J. W. Watson, *Green Chem.* **2012**, *14*, 251–259; b) R. Sheldon, Introduction to Green Chemistry, Organic Synthesis, and Pharmaceuticals. In Green Chemistry in the Pharmaceutical Industry, Wiley-VCH Verlag GmbH & Co. KGaA: **2010**; pp 1-20.

[2] a) P. Anastas, N. Eghbali, *Chem. Soc. Rev.* **2010**, *39*, 301–312; b) M. B. Gawande, V. D. Bonifacio, R. Luque, P. S. Branco, R. S. Varma, *Chem. Soc. Rev.* **2013**, *42*, 5522–5551.

[3] a) V. Polshettiwar, R. S. Varma, *Green chem.* **2010**, *12*, 743–754; b) Y. Liu, G. Zhao, D. Wang, Y. Li, *NatL. Sci. Rev.* **2015**, *2*, 150–166; c) M. Kidwai, Nanoparticles in Green Catalysis. In Handbook of Green Chemistry, Wiley-VCH Verlag GmbH & Co. KGaA: **2010**; d) J. A. Glaser, *Clean Tech. Environ. Policy* **2012**, *14*, 513–520; e) C. Ge, X. Sang, W. Yao, L. Zhang, D. Wang, *Green Chem* **2018**, *20*, 1805–1812; f) Z. Xu, X. Yu, X. Sang, D. Wang, *Green Chem* **2018**, *20*, 2571–2577.

[4] T. V. T. Phan, C. Gallardo, J. Mane, *Green Chem.* **2015**, *17*, 2846–2852.

[5] a) W. Zhang, G. Lu, C. Cui, Y. Liu, S. Li, W. Yan, C. Xing, Y. R. Chi, Y. Yang, F. Huo, *Adv. Mater.* **2014**, *26*, 4056–4060; b) P. Bera, M. S. Hegde, *RSC Adv.* **2015**, *5*, 94949–94979; c) X. Liu, J. Iocozzia, Y. Wang, X. Cui, Y. Chen, S. Zhao, Z. Li, Z. Lin, *Energy Environ. Sci.* **2017**, *10*, 402–434; d) M. B. Griffin, G. A. Ferguson, D. A. Ruddy, M. J. Biddy, G. T. Beckham, J. A. Schaidle, *ACS Catal.* **2016**, *6*, 2715–2727; e) X. Zhang, Z. Sun, B. Wang, Y. Tang, L. Nguyen, Y. Li, F. F. Tao, *J. Am. Chem. Soc.* **2018**, *140*, 954–962.

[6] a) A. Corma, H. Garcia, *Chem. Soc. Rev.* **2008**, *37*, 2096–2126; b) S. E. Davis, M. S. Ide, R. J. Davis, *Green Chem.* **2013**, *15*, 17–45; c) M. B. Gawande, A. Velhinho, I. D. Nogueira, C. A. A. Ghumman, O. Teodoro, P. S. Branco, *Rsc Adv.*, **2012**, *2*, 6144–6149; d) R. van Heerbeek, P. C. J. Kamer, P. van Leeuwen, J. N. H. Reek, *Chem. Rev.* **2002**, *102*, 3717–3756; e) M. B. Gawande, S. N. Shelke, P. S. Branco, A. Rathi, R. K. Pandey, *Appl. Organomet. Chem.* **2012**, *26*, 395–447; f) M. B. Gawande, R. K. Pandey, R. V. Jayaram, *Catal. Sci. Technol.* **2012**, *2*, 1113–1125; g) A. Schatz, O. Reiser, W. J. Stark, *Chem. Eur. J.* **2010**, *16*, 8950–8967; h) S. S. Li; L. Tao, F. Z. Wang, Y. M. Liu, *Y. Cao Adv. Synth. Catal.* **2016**, *358*, 1410–1416.

[7] a) J. C. Bauer, G. M. Veith, L. F. Allard, Y. Oyola, S. H. Overbury, S. Dai, *ACS Catal.* **2012**, *2*, 2537–2546; b) T. Risse, S. Shaikhutdinov, N. Nilius, M. Sterrer, H.-J. Freund, *Acc. Chem. Res.* 2008, 41, 949–956.

[8] a) M. Grzelczak, J. Perez-Juste, P. Mulvaney, L. M. Liz-Marzan, *Chem. Soc. Rev.* **2008**, *37*, 1783–1791; b) Z. Ma, S. Dai, *ACS Catal.* **2011**, *1*, 805–818; c) H. Liu, Y. Feng, D. Chen, C. Li, P. Cui, *J. Yang, J. Mater. Chem. A* **2015**, *3*, 3182–3223.

[9] a) S. J. Tauster, *Acc. Chem. Res.,* **1987**, *20*, 389–394; b) V. H. Mueller, M. P. Duduković, C. S. Lo, *Appl. Catal. A. Gen.,* **2014**, *488*, 138–147; c) C. J. Pan, M. C. Tsai, W. N. Su, J. Rick, N. G. Akalework, A. K. Agegnehu, S. Y. Cheng, B. J. Hwanga, *J. Taiwan Inst. Chem. Eng.* **2017**, *74*, 154–186; d) E. V. Golubina, E. S. Lokteva, A. V. Erokhin, A. A. Veligzhanin, Ya. V. Zubavichus, V. A. Likholobov, V. V. Lunin, *J. Catal.* **2016**, *344*, 90–99.

[10] a) A. V Kachynski, A. N Kuzmin, M. Nyk, I. Roy, P. N. Prasad, *J. Phys. Chem. C* **2008**, *112*, 10721–10724; b) C. Klingshirn, *ChemPhysChem* **2007**, *8*, 782–803; c) Z. L. Wang, *Mater. Today* **2004**, *7*, 26–33; d) P. X Gao, Z. L. Wang, *J. Am. Chem. Soc.* **2003**, *125*, 11299–11305.

[11] a) X. Song, H. Sun, X. Cao, Z. Wang, D. Zhao, J. Sun, H. Zhang, Xi. Li, *RSC Adv.* **2016**, *6*, 112451–112454; b) U. C. Rajesh, J. Wang, S. Prescott, T. Tsuzuki, D. S. Rawat, *ACS Sustainable Chem. Eng.* **2015**, *3*, 9–18; c) I. Chauhan, S. Aggrawal, P. Mohanty, *Environ. Sci.: Nano* **2015**, *2*, 273–279; d) B. Su, Y. Dong, Z. Jin, Q. Wang, Z. Lei, *Ceramics International* **2016**, *42*, 7632.

[12] a) A. K. Giri, A. Sinhamahapatra, S. Prakash, J. Chaudhari, V. K. Shahi, A. B. Panda, *J. Mater. Chem. A* **2013**, *1*, 814–822; b) A. K. Giri, A. Saha, A. Mondal, S. C. Ghosh, S. Kundu, A. B. Panda, *RSC Adv.* **2015**, *5*, 102134–102142; c) J. Li, H. Fan, X. Jia, *J. Phys. Chem. C* **2010**, *114*, 14684–14691; d) M. Wang, Z. Jin, M. Liu, G. Jiang, H. Lu, Q. Zhang, J. Ju, Y. Tang, *RSC Adv.* **2017**, *7*, 32528–32535; e) G. M. Oguz, C. Ozgur, A. Hatem, *J. Nanoscience Nanotechnol* **2012**, *12*, 9118–9124; f) M. Prabhu, J. Mayandi, R. N. Mariammal, V. Vishnukanthan, J. M. Pearce, N. Soundararajan, K. Ramachandran, *Mater. Res. Express* **2015**, *2*, 066202.

[13] a) A. Sinhamahapatra, A. K. Giri, P. Pal, S. K. Pahari, H. C. Bajaj, A. B. Panda, *J. Mater. Chem.* **2012**, *22*, 17227–17235; b) B. V. Kumar, H. S. B. Naik, D. K. Girija, *J. Chem. Sci.* **2011**, *123*, 615–621; c) M. Hosseini-Sarvari, H. Sharghi, *J. Org. Chem.* **2006**, *71*, 6652–6654.

[14] a) P. Pal, S. K. Pahari, A. K. Giri, S. Pal, H. C. Bajaj, A. B. Panda, *J. Mater. Chem. A* **2013**, *1*, 10251–10258; b) A. Sinhamahapatra, N. Sutradhar, B. Roy, P. Pal, H. C. Bajaj, A. B. Panda, Appl. Catal. B: Env. **2011**, *103*, 378–387; c) B. Karmakar, A. Sinhamahapatra, A. B. Panda, J. Banerji, B. Chowdhury, Appl. Catal. A: Gen. **2011**, *392*, 111–117; d) H. Singh, P. Pal, C. Sen, A. B. Panda, S. C. Ghosh, *Asian J. Org. Chem,* **2017**, *6*, 702-706; e) C. Sen, T. Sahoo, S. M. Galani, A. B. Panda, S. C. Ghosh, *ChemistrySelect* **2016**, *1*, 2542–2547.

[15] a) S. Wunder, F. Polzer, Y. Lu, Y. Mei, M. Ballauff, *J. Phys. Chem. C* **2010**, *114*, 8814; b) T. Aditya, A. Pal, T. Pal, *Chem. Commun.* **2015**, *51*, 9410.

[16] a) X.; Wan, W. Deng, Q. Zhang, Y. Wang, *Catal. Today* **2014**, 233, 147–154; b) K. Suzuki, T. Yamaguchi, K. Matsushita, C. Iitsuka, J. Miura, T. Akaogi, H. Ishida, *ACS Catal.* **2013**, *3*, 1845-1849; c) R. K.; Sharma, S. Gulati, *J. Mol. Catal. A: Chem.* **2012**, *363–364*, 291–303.

[17] J. C. C. Fan, J. B. Goodenough, *J. Appl. Phys.* **1977**, *48*, 3524–3531.

[18] S. M. Park, T. Ikegami, K. Ebihara, *Thin Solid Films* **2006**, *513*, 90–94.

[19] M. Chen, X. Wang, Y. H. Yu, Z. L. Pei, X. D. Bai, C. Sun, R. F. Huang, L. S. Wen, *Appl. Surf. Sci.* **2000**, *158*, 134–140.

[20] L. K. Ono, B. R. Cuenya, *J. Phys. Chem. C* **2008**, *112*, 4676-4686.

[21] A. Naitabdi, L. K. Ono, F. Behafarid, B. R. Cuenya, *J. Phys. Chem. C* **2009**, *113*, 1433–1446.

[22] a) P. Prakash, D. D. Masi, V. Geertsen, F. Miserque, H. Li, I. N. N. Namboothiri, E. Gravel, E. Doris, *ChemistrySelect* **2017**, *2*, 5891–5894; b) J. Chauhan, S. Fletcher, *Tetrahedron Lett.* **2012**, *53*, 4951–4954

Submitted: June 7, 2018
Accepted: August 16, 2018